Engineering Structures 339 (2025) 120647

Contents lists available at ScienceDirect

Engineering Structures

journal homepage: www.elsevier.com/locate/engstruct

Long-term viscous effects of in-field tests on HDRBs-based seismic isolation systems

Laura Ragni [a,*], Fabio Micozzi [b], Andrea Dall'Asta [b]

[a] Department of Civil and Building Engineering and Architecture, Università Politecnica delle Marche, Italy
[b] School of Science and Technology, University of Camerino, Italy

ARTICLE INFO

Keywords:
Hybrid base-isolation system
HDRBs
Viscous effects
Full-scale tests
Push-and-release tests

ABSTRACT

Push and release tests on full-scale base-isolated buildings can be considered de facto as in situ verification tests of the actual behaviour of a base-isolation system. However, for isolation systems based on High Damping Rubber Bearings (HDRBs) the test response significantly depends on the pushing phase velocity. If this is quite low (due to the limited capacity of the hydraulic system), the free vibration response can remarkably differ from the expected one (considering nominal properties of HDRBs) due to the viscous behaviour of HDR compounds. Therefore, a model that adequately describes the viscous effects related to different strain velocities is crucial for correctly interpreting the experimental measurements obtained from the tests. This paper examines in detail the viscous effects observed in both laboratory tests conducted on a couple of HDRBs (type tests) and the experimental in-situ tests performed on a base-isolated structure equipped with an hybrid system comprising HDRBs and Low Friction Sliders (LFSs). A simple linear viscoelastic model of the HDRBs is developed based on type tests and then used to simulate the base-isolation system response. Results show that the model effectively predicts the experimental response (the pushing phase, the free vibration response and the final residual displacement) and that it can be used to verify that nominal properties of HDRBs (as well as friction of LFSs) are consistent with the design specifications, even if the recorded response differs from the expected one considering those parameters.

1. Introduction

High Damping Rubber Bearings (HDRBs), unlike Natural Rubber Bearings (NRBs), may exhibit viscous effects depending on the rubber compound used in their manufacturing, which can result in velocity-sensitive behavior. Specifically, two distinct effects can be identified: those occurring at high velocities (within the range of dynamic excitations) and those at low velocities (within the range of quasi-static actions), referred to as short-term and long-term effects, respectively [1–4]. This implies that the seismic response of HDRBs (influenced by the short-term viscosity only) may be significantly different form the response to low-velocity loading histories, where the long-term viscosity and the associated stress loss become predominant [2]. Conversely, within the range of seismic velocities, the sensitivity to velocity variations is limited, as recently investigated and experimentally demonstrated also for unbonded fiber reinforced elastomeric isolators (UFREIs) made by high damping rubber [5]. Consequently, when conducting push and release tests on real scale base-isolated buildings equipped with HDRBs, the dynamic response of the building will mirror to the expected behaviour under seismic excitations only in if the pushing phase is sufficiently rapid. Conversely, if the pushing phase is considerably lower than the velocities involved in the release phase (due to the limited hydraulic capacity of the in-situ pushing system), the subsequent free motion will be notably influenced by the long-term viscosity, i.e. by the stress loss occurring during the loading phase. The loading velocity mainly depends on the capacity of the hydraulic system available for on-site tests and the dimension of the structure. Typically the hydraulic power available during in-field tests are lower compared to laboratory tests. On the other side, the forces required are much higher as all the bearings are tested simultaneously. Both these conditions usually lead to very low loading speeds.

In light of this specificity, this article first presents a detailed analysis of the tests conducted over time on base-isolated buildings incorporating HDRBs [6–10], with emphasis on the pushing system, building dimensions and observed response. Then, the experimental campaign recently carried out on the CHIP (CHemistry Interdisciplinary Project) building by the same authors is analyzed in detail, with particular attention to the viscous effects observed during the tests and with the

* Corresponding author.
E-mail address: laura.ragni@univpm.it (L. Ragni).

https://doi.org/10.1016/j.engstruct.2025.120647
Received 1 February 2025; Received in revised form 24 April 2025; Accepted 22 May 2025
Available online 30 May 2025
0141-0296/

aim of correctly interpreting the experimental results, for which all data are available. The CHIP building is a two-storey steel braced frame structure seismically protected by means of an hybrid isolation system, consisting of HDRBs and Low Friction Sliding Bearings (LFSBs), More in detail, the building design and geometry, as well as the base-isolation system, are described in [11], whereas the design of the experimental campaign and main results regarding both the base-isolation system and the superstructure are illustrated in [12]. Here experimental results of interest to characterize the viscous behaviour of HDRBs are critically analysed and discussed, also including laboratory tests carried out during the qualification phase of the bearings (type tests), where short-term and long-term viscous contributions may be separately evaluated. Then, a simple linear viscoelastic model is used to interpretate the tests. At this regards it should be noted that the choice of a simple as possible model has been made for two reasons: (i) to demonstrate that the main deviations between the experimental response and the seismic one concern the slow rate viscosity only (thus demonstrating that other nonlinear phenomena provide marginal contributions) and (ii) to provide a practical tool that can be easy calibrated combining on-site tests with type tests on the devices. More advanced models developed over the time for HDRBs, would require very complex calibration procedures [1] or they would not be functional since oriented to simulate the seismic response neglecting the velocity-dependent behaviour [2–5].

More in detail, starting from the type tests, a simple linear viscoelastic model of a single HDRB has been defined and then used to simulate the behaviour of the entire base-isolation system, by also adding the friction contribution of sliders. The model for HDRBs, consisting of a Maxwell model in parallel with a Kelvin, is able to compute the viscous displacement (lost displacement) accumulated during the slow loading phase and to simulate the release phase where the system oscillates around a non-zero displacement. The final (residual) displacement can be also correctly estimated, as the long term viscous effect has vanished, by demonstrating the recentring capacity of the isolation system if the friction force of the sliders is sufficiently low. In the field of seismic velocities, the Maxwell model behaves almost like an elastic spring, whose stiffness, added to the Kelvin model one, provides the nominal dynamic stiffness of the isolator. Therefore, for seismic applications the proposed model coincides with the equivalent linear model proposed by all standards [13,14] and verified in [15], while simultaneously being able to simulate the behaviour at low velocities typical of quasi-static loading paths.

It is worth to notice that this kind of in-field tests on base-isolated buildings are of particular interest since, according to European and national Standards [13,14], quality control test are not required for LFSBs and performed only on the 20 % of installed HDRBs. As already highlight in [16], this can represent a drawback, due to the essential role of the isolation system on the seismic behaviour of the building. However, testing all the devices it would be expensive and it would completely disregard the real in-situ condition of bearings after their installation. Thus, testing the all isolation system through in-field push and release tests is an interesting way to assess the isolation-system reliability, especially for strategic buildings. In this context, the proposed model and the associated procedure used to define its parameters (including the friction force of LFSBs) is an essential tool to interpretate the response to this kind of in situ verification tests and to demonstrate how the parameters involved in the recorded response are coherent with the design requirements (nominal design parameters of HDRBs and design friction force of LFSBs).

2. Literature review about in-field tests on HDRB-based seismic isolation systems

In the European context, HDRBs are commonly used due to their intrinsic dissipative capacity since ’90 and various full scale tests on base-isolated buildings have been conducted since their initial applications in "all-rubber" isolation systems, and later, in hybrid isolation systems where they are used with LFSBs. In Italy, the first full-scale test dates back to 1991 [6] and it was conducted with explosive charges for the release, but documentation on this test is limited. Later, two tests were carried out: the first in Potenza in 1997 [7] and the second in Rapolla in 2000 [8], using the same device designed to reduce the forces involved. It consists of a three-hinged arch pulled vertically by jacks, which, when approaching the straight configuration, becomes unstable. The in building Potenza is of considerable size (plan area of 2200 m^2 and an occupied volume of 44000 m^3) with 89 HDRBs, thus the loading speed was necessarily slow, even if not documented in the paper, and the free vibration motion consists in few oscillations around a non-zero displacement that is slowly recovered over time, as shown later in the paper for the CHIP building. The same device was then used in 2000 for a residential building in Rapolla. In this case the building was significantly smaller as well as the number of isolators (28 or 16 depending on the tested configuration) and it showed a free vibration motion with a larger number of vibration around its initial position. Successively, two tests were carried out using a pushing device very similar to that one used in the tests described in this paper. The first one [9] was conducted in 2004 on a four-story residential building of modest dimensions located in Solarino (Sicily, Italy), which was isolated with 12 HDRBs and 13 LFSBs. Subsequently, in 2013, the same device was used to test a larger building at Augusta [10], isolated at the base with 16 HDRBs and 13 LFSBs. While on the first building there is little documentation, there are several documents on the second building, and particularly in [10] it is clearly shown that the loading rate of the pushing phases is low in this case (approximately 0.11 mm/s, as can ben deduced by figure 1.10 of [10]), and the resulting free vibration motions (figures 1.12 and 1.13 of [10]) are very similar to those later shown in this paper, i.e. characterized by few oscillations around a residual displacement that is recovered very slowly over time. However, in none of the aforementioned articles where the phenomenon was observed an analysis on the viscous effects typical of HDRBs has been conducted. This analysis was instead possible on the tests illustrated below related to the CHIP building, for which all required data are available.

3. Experimental tests conducted on the CHIP building

This section collects experimental tests carried out on a couple of HDRBs during their production (type tests) and in-field tests carried out on the base-isolated building. In particular, a brief description of the base-isolated building and the experimental set-up is first reported, then type tests on the bearings are described in detail and finally the in-field static and dynamic tests are summarized by focusing on the effects due to the viscous behaviour of HDRBs.

3.1. Base-isolated building and testing set-up

The tested building is the new research centre of the University of Camerino called ChIP (Chemistry Interdisciplinary Project), hosting chemistry and physics laboratories. Its construction was funded by the Italian Department of Civil Protection (DPC) after the 2016–2017 Central Italy seismic sequence and it is a strategic building also intended as coordination centre of the DPC for future post-earthquake emergency phases. The superstructure is a steel braced frame with pinned joints, designed using a 7.2 m × 7.2 m modular system, for a total of 7 modules along each direction, plus a cantilever zone spanning 1.9 m along the entire perimeter of the building (Fig. 1). The reinforced concrete (RC) substructure consists of foundations at different levels and rigid columns connecting the deeper foundations to the isolation level. The isolation system consists of 28 HDRBs made of soft rubber (diameter 600 mm and total rubber height 184 mm) arranged on the perimeter and 36 LFSBs in the central part to support the higher vertical loads, designed by assuming a nominal isolation period Tis = 3.60 s. Further information regarding the design process can be found in [11].

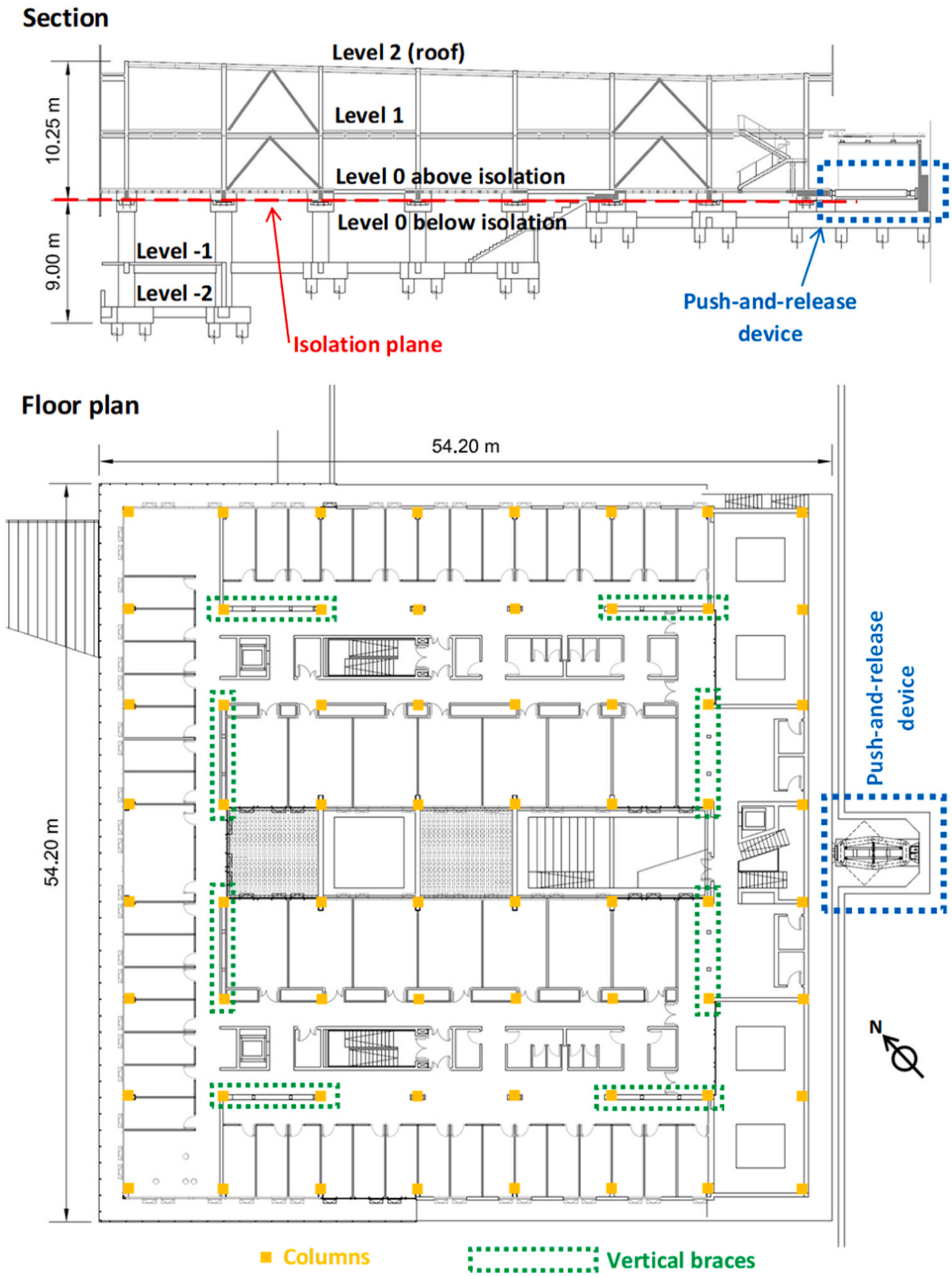

Fig. 1. Tested building in Camerino, Italy.

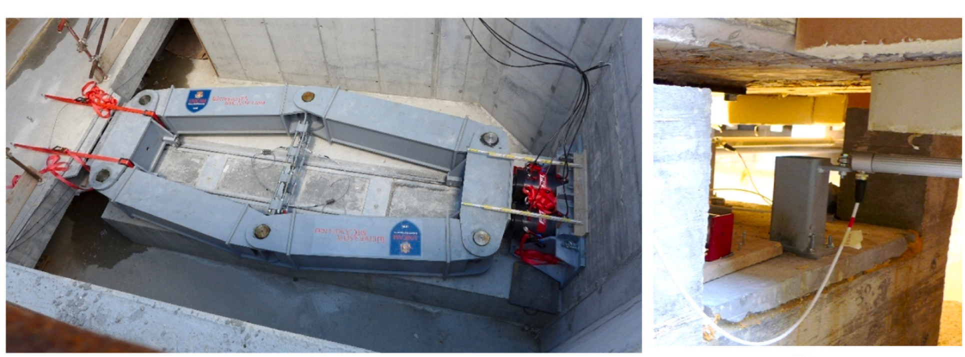

(a)   (b)

Fig. 2. Push-and-release device (a) and horizontal displacement sensors at level 0 (b).

As described in detail in [12], to carry out in-field experimental tests, a push and release device has been designed together with the building, consisting of a quadrilateral articulated steel system and relevant reaction structures (Fig. 2a). A high strength steel rod is inserted in the middle of the tie element of the quadrilateral system, working as a fuse. Two hydraulic jacks with maximum stroke of 300 mm and total maximum force of 10 MN and two load cells were positioned in series with the push and release device to apply and measure the pushing force. When the fuse breaks due to the tension force, the base-isolated building starts to oscillate in free-vibration conditions. However, as already mentioned in the introduction, if the capacity of the in-situ available hydraulic system is limited (maximum flow rate equal to 5 l/min) the loading rate of the pushing phase is low and this influences the following free vibration response. During the tests a full set of sensors was installed in the building to monitor all the relevant response parameters, however, in this paper data from horizontal displacement transducers at the isolation level (Fig. 2b) are only analysed. Detailed information about the sensors and their positioning can be found in reference [12].

3.2. Type tests of elastomeric devices

During the production of bearings, the European standard on anti-seismic devices [13] as well as the national seismic code [14] prescribe to perform type tests in order to verify that bearings proprieties agree with design prescriptions. Three different kinds of test are required: horizontal cyclic characterization (HCC) tests carried out at a frequency of 0.5 Hz and different displacements, a one side ramp (OSR) test carried out at the design displacement with a velocity of 5 mm/s (that is not mandatory and not performed in some cases) and lateral capacity (LC) tests. In the latter minimum and maximum axial loads are imposed to the bearings together with an increasing horizontal displacement up to a maximum value, then the displacement is then held constant for about 4 minutes before decreasing it. In Fig. 3a results of HCC tests are reported with different colours for different maximum shear strains γ imposed, showing two main effects. The first one, known as Payne effect [17], consists of a decreasing of the bearing stiffness as the maximum amplitude increases. The second one is the Mullins effect [18–20], i.e. the change of the hysteresis loops for repeated cycles up to a stable behaviour, which becomes more and more evident as the maximum attained displacement increases [1–3]. At this regard, seismic codes prescribe to consider third cycle data to determine nominal bearing properties [13,14,21]. According to this indication, in Fig. 4 the equivalent linear properties [22] in terms of shear modulus (G) and equivalent linear damping (ξ) are illustrated for the different displacement amplitudes tested. It is evident how the shear modulus varies significantly with the shear strain (γ) while the damping is almost constant. In Fig. 3b the HCC test at the design displacement has been compared with the OSR test at the same displacement amplitude to show the importance of the viscous behaviour, i.e. the dependence of the bearing response on the strain rate. The difference is related to a change in velocity from 5 mm/s (quasi-static) for OSR test up to 500 mm/s (dynamic range) for HCC tests. Finally, in Fig. 5 lateral capacity tests are reported in terms of force profile over time (Fig. 5a) and force-displacement loops (Fig. 5b). The OSR test is again reported for comparison purpose. Also in this case the viscous behaviour of the bearing is evident since the force notably decrease when the displacement is held constant.

3.3. In-situ experimental tests on the base-isolated building

In-situ experimental tests were performed when the steel structure was completed, before the installation of non-structural elements (partitions, external walls, architectural elements, and technological equipment). The total estimated mass of the structures above the isolators in such condition is 4634 tonnes. Two types of tests were conducted: 1) loading and unloading tests (without release), hereafter called quasi-static (S) tests; 2) loading tests (up to the rupture of the fuse) followed by a sudden release, hereafter called dynamic (D) tests. The sequence of the tests is reported in Table 1, indicating the maximum horizontal force and displacement attained as well as the residual displacement after 30 min the end of the test and at the start of the successive test. A complete description of the results of the experimental campaign is reported in [12], here, only a summary of results about the isolation system is provided. In particular, Fig. 6a shows displacement time histories, whereas Fig. 6b shows the corresponding force time histories measured by the load cells, where the force drop to zero only for dynamic tests. In both these figures, conventionally, the time was set to zero when the displacement decrement started (for the quasi static tests) and when the load cells recorded the drop of the applied horizontal (in the dynamic tests). It can be observed from the loading ramps that the loading rate is quite low, for example test D1 takes about 15 min to reach the maximum displacement, resulting in a load rate less than 0, 2 mm/s. It is specified that the control was purely manual and that a such low value is due to the limited capacity of the available hydraulic system (equal to 5 l//min). At the end of the pushing phase of dynamic tests obviously the force drop to zero and the displacement response is only recorded. Fig. 7 shows a zoom of the release phase of the dynamic tests, where the free vibration motion of the building can be observed in detail. It is evident that the system only makes few oscillations around a non-zero displacement that gradually decreases. As commented in detail in [12] at the end of the last test (S3), where the maximum displacement is imposed, the residual displacement is 36.2 mm (30 minutes after the initiation of the unloading phase, as indicated in Table 2). The recovery

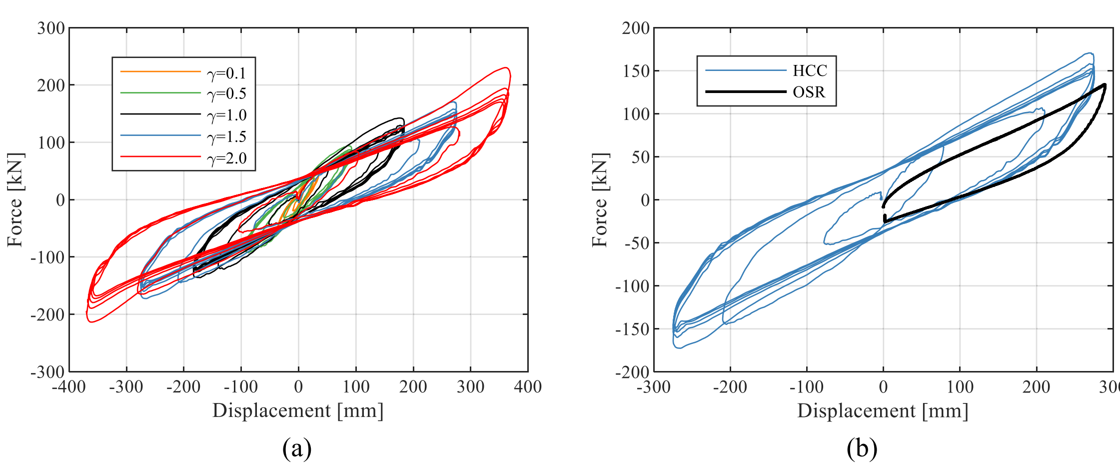

Fig. 3. HCC tests (a) and OSR test compared to the HCC test at the same displacement (b).

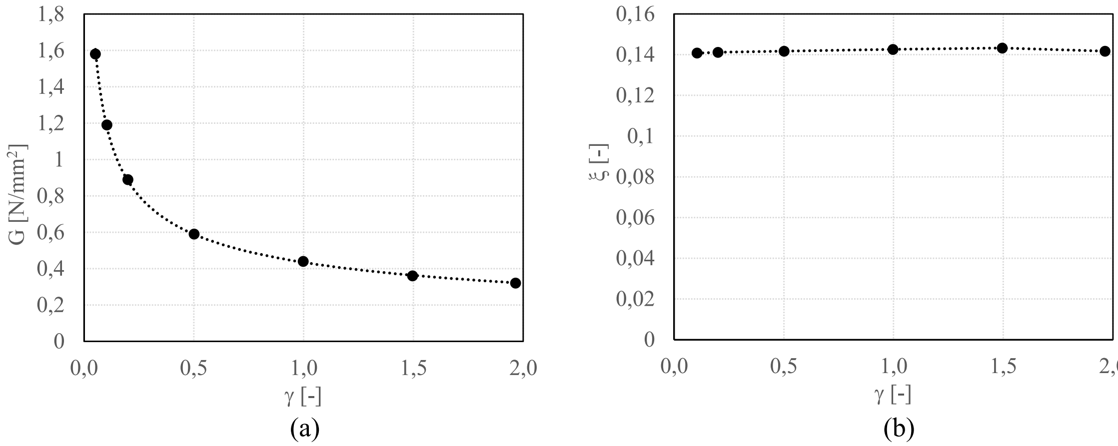

Fig. 4. Equivalent properties of HDRBs at different strain amplitudes: shear modulus (a) and damping coefficient (b).

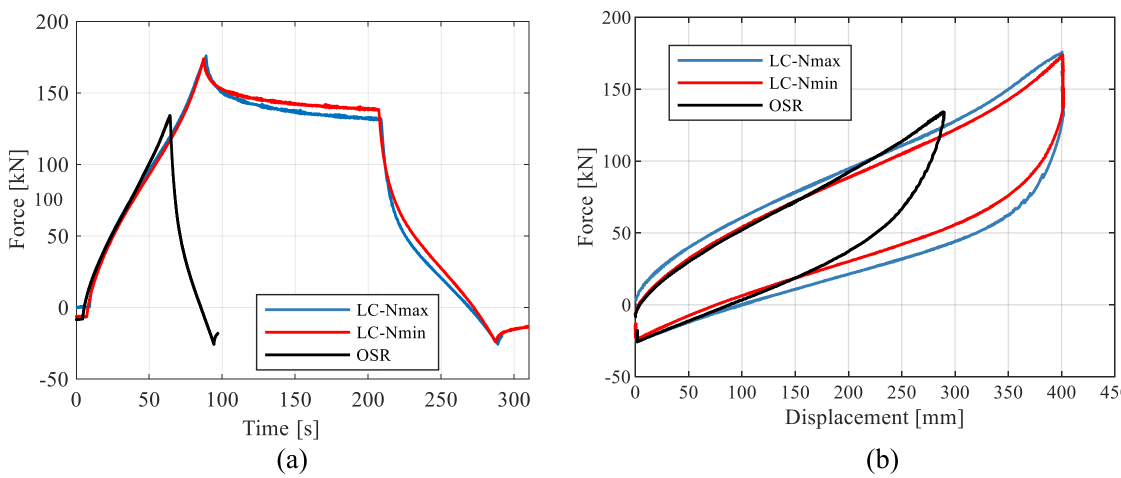

Fig. 5. Force vs time (a) and force-displacement diagram (b) of OSR test (black) and LC tests with minimum (red) and maximum (blue) axial loads.

Table 1
Tests sequence.

Day	Test	Starting time	Duration [min]	Max Force [kN]	Max displacement [mm]	Displacement at test start [mm]	Displacement 30 min after release/unloading start [mm]
3rd July 2020	A1	10:55	30	-	-	-	-
	S1	12:22	6	518	0.0	0.0	0.0
	D1	13:47	16	2729	177.3	0.0	15.7
	S2	16:36	21	3206	232.4	15.2	26.1
6th July 2020	A2	10:11	40	-	-	-	-
	D2	12:24	8	1756	109.4	22.1	22.4
	D3	13:36	18	3122	226.9	22.1	23.4
	A3	15:27	23	-	-	-	-
	D4	15:56	9	1786	121.8	22.1	22.9
	S3	17:07	25	3834	284.6	22.6	36.2

of the residual dis-placement, due to the viscous behaviour of the HDRBs, continued and after one month a final residual displacement equal to 25 mm was measured, in accordance with the expected friction force of the sliders. In [12] the horizontal force-displacement curves of these tests are also illustrated, by showing that the force during the release phase of dynamic tests (derived from the acceleration recorded at the isolation level and the mass of the structure) significantly differs from the force recorded during static tests. It is also shown that the loading ramp of the tests with largest displacements (S2, D3 and S3), once deducted of the dynamic friction force estimated (equal to 200 kN) and scaled with respect to a single HDRB, coincides with the OSR test (all in the quasi-static range of loading velocity) while a significantly differs from the HCC test, due again to the viscous behaviour of HDRBs.

4. Numerical simulation

4.1. Numerical model of the base-isolation system

Regarding the base-isolated building, a SDOF (Single-Degree-Of-Freedom-Model) model [23] has been adopted, neglecting the deformability of both the superstructure and substructure and modeling the base isolation system as a combination of three parallel elements (Fig. 8a). The first element is a Kelvin model (stiffness k_0 and damping constant c_0), the second one a Maxwell model (stiffness k_1 and damping

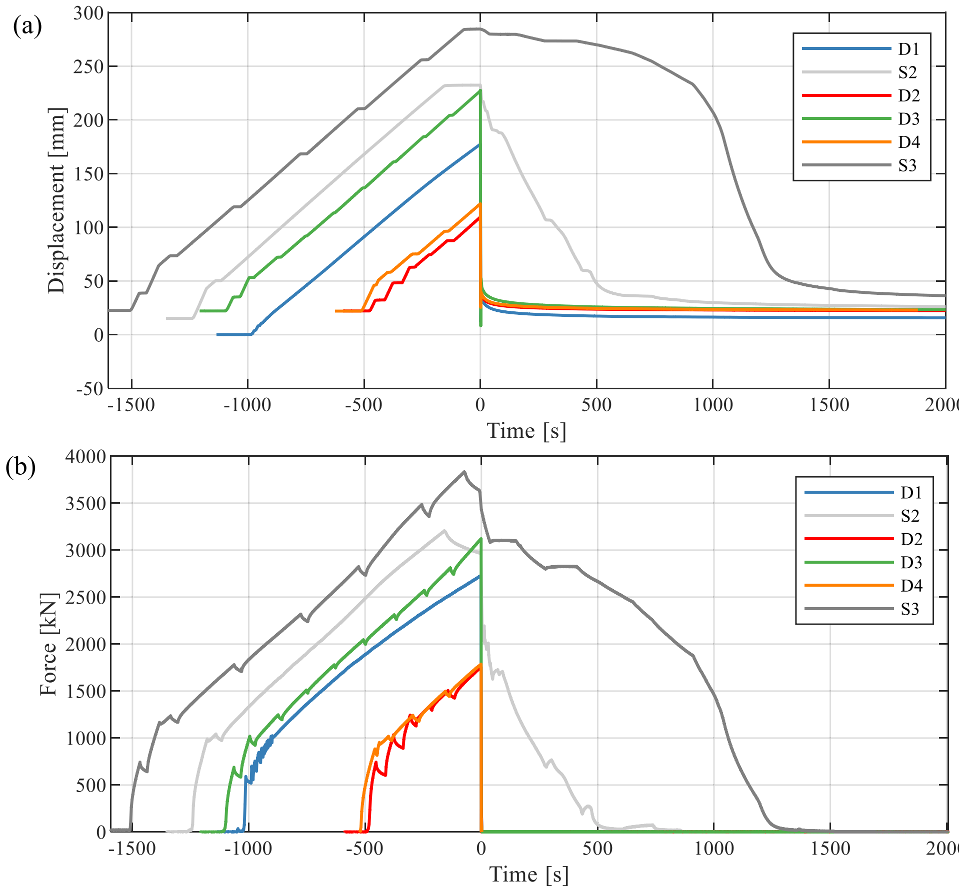

Fig. 6. Displacement (a) and force (b) time-history curves of dynamic and static tests.

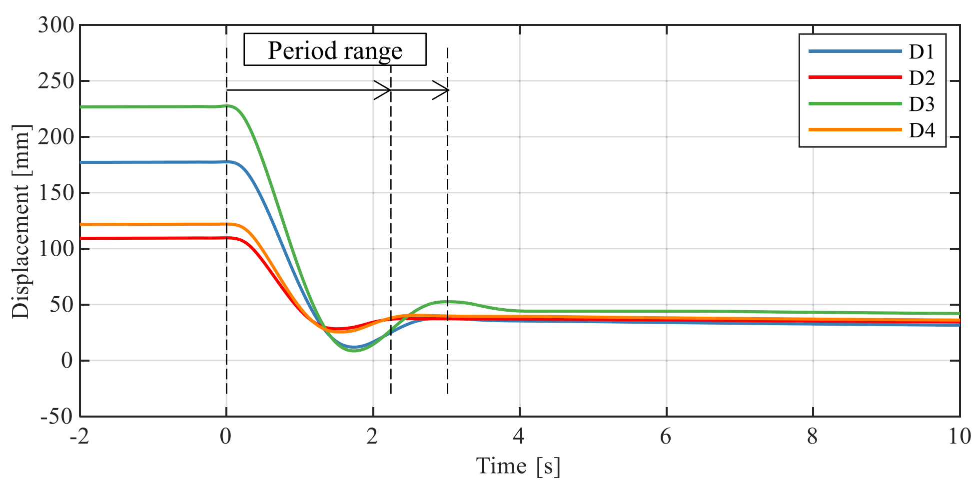

Fig. 7. Displacement time-history curves of the release phase of dynamic tests.

Table 2
Model parameters of a single HDR bearing.

γ_{is} [-]	$G(\gamma_{is})$ [N/mm^2]	$k_{1,is}$ [kN/m]	$c_{1,is}$ [kNs/m]	$k_{0,is}$ [kN/m]	$c_{0,is}$ [kNs/m]
2.18	0.307	150	840	323	42

constant c_1) and the last one is a friction model characterized by a constant friction force F_{fr}. The first two elements simulate the response of HDRBs, while the latter represents the contribution of LFSBs. This is the simplest model that allows to describe the viscous effects of HDRBs illustrated in the previous section (once the friction force F_{fr} is exceeded). More in detail, by combining Kelvin and Maxwell models and by properly setting the relevant viscous constant (c_0 and c_1) the twofold viscous behaviour, i.e. short-term and long-term viscous effects, can be described. Specifically, if the displacement rate ($\dot{u}$) is low the response is controlled by the Maxwell model and the long-terms viscous effect is predominant. In this case in fact the displacement "lost" in the damper (lost displacement u_1) is large and the displacement of the spring of the Maxwell model (u-u_1) is lower than the imposed displacement (u). Consequently, the global stiffness is low, tending to k_0 for very small

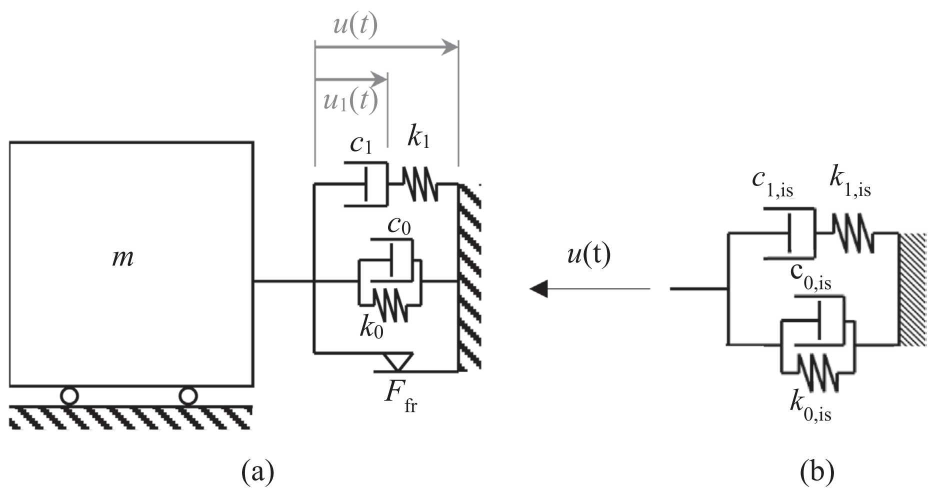

Fig. 8. Numerical model of the isolation system (a) and the single HDRB (b).

velocities, and the lost displacement is large and slowly recovered over time at the end of the excitation, according to the fading memory viscoelasticity theory [24]. On the other hand, if the displacement rate is sufficiently high the reaction of the damper of the Maxwell model is very large and the relevant lost displacement is low. In this case there are no displacements to recover and the global stiffness is close to the sum of the stiffnesses of both the elements ($k_0 + k_1$), that coincides with the nominal stiffness of the bearings. For even higher velocities, damping increases but stiffness does not increase further. In mathematical terms, the equilibrium equation of the dynamic system depicted in Fig. 8a and the evolution low of the internal variable u_1 are described by the following equations:

$$\ddot{u} = -\left(k_0 u + c_0 v + k_1(u - u_1) + (F_{fr}\mathrm{sgn}(v)\right)/m \tag{1a}$$

$$\dot{u}_1 = k_1(u - u_1)/c_1 \tag{1b}$$

where $v = \dot{u}$ is the velocity of the system and F_{fr} the total friction force of sliders. Despite its simplicity, the model is adequate to catch the most relevant phenomena involved in the response of push and release tests. The main simplifying assumption is the linear behaviour of HDRBs; however, as shown in the next section, the simulated response obtained is very close to the experimental one for this application, Moreover, the nonlinear extension could be easy implemented, if needed.

In the following section, the model parameters referring to a single HDRB (shown in Fig. 8b) have been first computed based on type tests. Then, that model has been used to simulate the base-isolated building response, also accounting for the friction forces due to sliders. Since type tests on sliders are usually not required by the codes (when their role is not to dissipate energy but only to support vertical loads, as specified in [13]), the total friction force from in-situ tests has been considered, as identified in [12].

4.2. HDR bearing model based on type tests

With regard to the single bearing model (Fig. 8b) the following hypotheses have been made to compute the parameters of Maxwell and Kelvin elements: (i) the velocity of the HCC test is such that the lost displacement is zero and (ii) the force recorded at the end of the constant displacement path of the LC test is representative of the Kelvin element stiffness (i.e. elastic stiffness). Consequently, the nominal stiffness (for seismic applications) of a single bearing ($k_{n,is}$) coincides with the equivalent stiffness of the HCC test and can be computed as the sum of the stiffness of the Maxwell and Kelvin elements ($k_{1,is}$+$k_{0,is}$), as reported in the following expression:

$$k_{n,is} = G\ A_{is}\ /\ h_{is} = k_{1,is} + k_{0,is} \tag{2}$$

where $A_{is} = 0.2827\ m^2$ (corresponding to $D_{is} = 0.6$ m), $h_{is} = 0.184$ m. According to Fig. 4a, the shear modulus G can be calculated as a function of the shear strain (γ) by means of the following expression:

$$G = 0.434\ \gamma^{\ (-0.45)} \tag{3}$$

Since G is assumed to be constant in the linear model, for each tests the value corresponding to the maximum shear strain amplitude attained has been calculated and set in the model. The viscous constant of the Kelvin model of the single bearing ($c_{0,is}$) has been estimated from the equivalent damping ratio of the HCC test, that is $\xi = 0.14$ (Fig. 4b) regardless the shear deformation, by using the following formula:

$$c_{0,is} = \frac{2\xi k_{n,is}}{\omega} \tag{4}$$

where ω= 2πf with f= 0.5 Hz. Conversely, the Maxell model parameters (always referring to a single bearing) can be derived from the LC tests. More in detail, $k_{1,is}$ has been computed as the ratio between the force at the end of the constant displacement path (limit force or elastic force) and the corresponding displacement, while $c_{1,is}$ has been obtained by fitting (on average) the diagram of the total force over the time, as depicted in Fig. 9a. The lost displacement simulated by the model during the slow loading phase is depicted in Fig. 9b, together with the imposed displacement. Obviously, peaks (as well as valley) of the force time history cannot be simulated by a such linear model. However, as shown later on, the ability of this linear model in simulating the experimental results is quite accurate. Thus it can be considered a very simple and useful tool to interpret results of in-situ tests, which is the aim of the paper. Finally, the difference between the nominal stiffness and the stiffness of the Maxwell model gives the stiffness of the Kelvin model ($k_{0,is}$).

The obtained parameters referring to the single bearing model reported in Fig. 8b are reported in Table 2, where the maximum shear strain (γ_{is}) of the tests and the corresponding value of the shear modulus are also reported. Force-displacement cycles of the HCC tests are also numerically simulated and results are reported in Fig. 10a for the test carried out at the maximum displacement, by considering the third cycle only of the experimental data. The shape of cycles are notably different because the linear model proposed can't provide a better fitting of both the OSR and HCC tests. However the difference in the dissipated energy (area of cycles in Fig. 10a) is about 10 %. Despite these differences, as illustrated in the next section, the proposed model is capable of simulating the release tests with a satisfactory level of accuracy, as equivalent stiffness, damping and viscous displacement are correctly defined. Naturally, with a more complex model, such as the one proposed in [1],

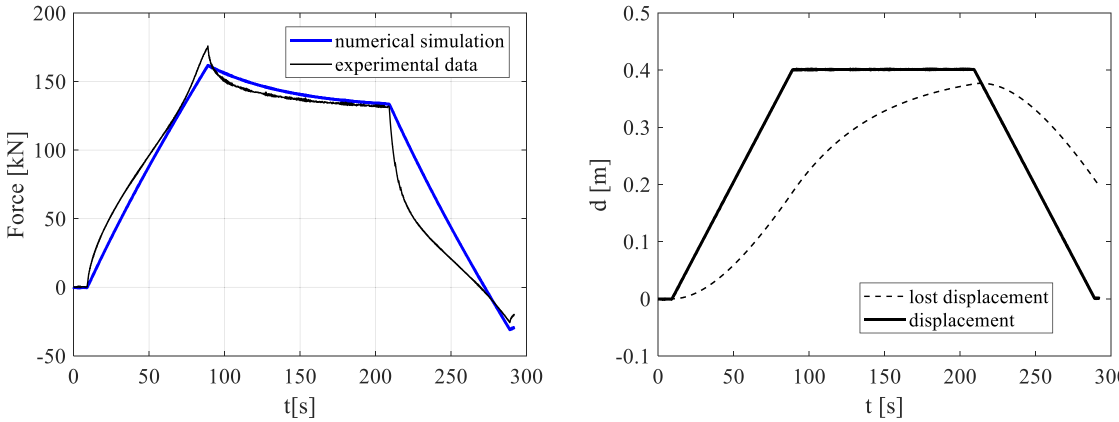

(a) (b)

Fig. 9. Numerical simulation of force vs time (a) and lost displacement (b) of the OSR test.

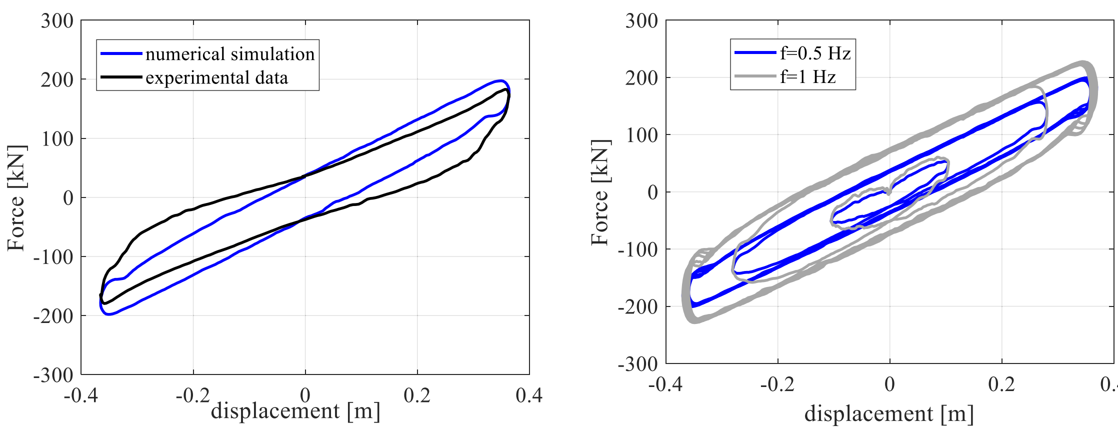

(a) (b)

Fig. 10. Numerical simulation of force-displacement cycles of HCC tests at 0.5 Hz (a) and numerical cycles at 0.5 Hz and 1 Hz (b).

an even more accurate simulation would have been obtained, but with a significantly higher number of parameters to calibrate. Finally, in Fig. 10b the simulation of the HCC test with an increased velocity (f=1 Hz) is reported to show the velocity dependent behaviour of the model in the range of seismic applications (short term viscosity).

4.3. Simulation of in situ-tests

To obtain the parameters of the numerical model reported in Fig. 10a, simulating the response of the whole base-isolated building, parameters reported in Table 2 should be modified according to the maximum displacement attained during each test and then multiplied by the number of HDRBs (28 in this project). Results are reported in Table 3 together with the maximum shear strain (γ_{is}) and the corresponding shear modulus (G) used to obtain the model parameters. Furthermore, the total friction force provided by the sliders needs to be evaluated. At this regard, the dynamic friction force has been obtained from the inversion point of the force-displacement diagram of the quasi-static tests, as illustrated in [12]. The obtained value is F_{fr}= 300 kN for the first test (D1) and F_{fr}= 200 kN for all the other tests, but a breakaway force a little larger than the dynamic friction force has been assumed to simulate the initial loading ramp (assumed values are 500 kN for the test D1 and 300 kN for all the other tests), as experimentally observed and explained in [12]. For example, in Fig. 11a the loading phase of D2 test is simulated and compared with the experimental results. It is evident how, once the breakaway force is exceeded, the model is able to simulate the viscous effects occurring during the loading phase, where the displacement is left constant for some time intervals to register the force decrement (Fig. 11a). From Fig. 11b it can be seen that the lost displacement computed by the model (u_1) is close to the imposed one (u), confirming that the loading rate is very low (for this rubber compound). In Fig. 12 the free vibration motion after the release is reported for all the dynamic tests (D1, D2, D3 and D4) by comparing model data (red continuous line) and experimental data (black dashed line). For all

Table 3
Model parameters of the base-isolated building.

Test	γ_{is} [-]	$G(\gamma_{is})$ [N/mm^2]	k_1 [kN/m]	c_1 [kNs/m]	k_0 [kN/m]	c_0 [kNs/m]	ξ [-]	T_{is} [s]	T_{test} [s]
D1	0.96	0.353	6137	469866	9054	2349	0.14	3.47	2.95
D2	0.60	0.436	9742	522650	9054	2613	0.14	3.12	2.50
D3	1.24	0.355	5406	458421	9054	2292	0.14	3.56	3.00
D4	0.66	0.416	8873	510421	9054	2552	0.14	3.19	2.65

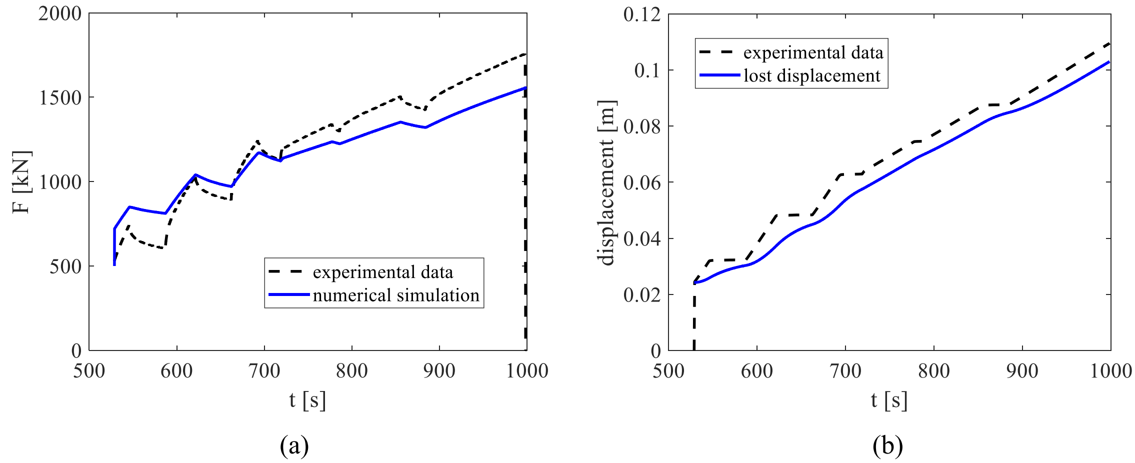

Fig. 11. Numerical simulation of force vs time (a) and displacement and lost displacement vs time (b) of the loading phase of test D2.

of them the first column shows the motion just after the release (from 0 s to10s), while the second column shows the displacement at long term (from 100 s to1000s). First of all, it can be observed that the building experiences only one oscillation around a non-zero displacement; then the displacement decreases gradually over time. This is due to the displacement absorbed by the Maxwell model during the loading phase that causes a viscous overstress during the release phase leading the isolation system to oscillate around a non-zero position. To show this, the lost displacement of the numerical model (u_1) is also reported in Fig. 12 (blue continuous line) together with the total displacement (u). It can be seen that the numerical simulation is very close to the experimental data both at short term (just after the release) and at long term, when the displacement and lost displacement gradually decrease. At short term, the error in estimating the minimum displacement with respect to the initial one (u_0-u_{min}) has been computed as the difference between experimental and numerical values with respect the experimental one ($E_{u,min}$). Obtained values are all lower than 10 %. After the minimum displacement peak the difference between experimental and numerical results are evident only for test D3 (where the largest displacement is attained), due to the assumption of linear model that cannot simulate the stiffer behaviour at shear strain much smaller that the shear strain assumed for its calibration. However, these differences goes to zero after a sufficient time period. At long term, final residual displacement computed by the model is very close to the measured one (approximately 25 mm for both experimental data and numerical simulations) and is determined by the balance between the elastic response of the HDRBs and the friction force of the LFSBs once over-stresses are fully dissipated.

Fig. 13 shows the comparison between model and experimental data in terms global velocity ($\dot{u}$). The lost velocity ($\dot{u}_1$) related to the Maxwell component is also shown. Once again the simulated responses are in good agreement with the measured ones, as demonstrated by the computed Root Square Mean Error (RMSE). The velocity time histories clearly show the period of the base isolated building, that can be roughly estimated as the time interval from the begin of the motion and the end of the first velocity cycle (corresponding to the positive displacement peak). By considering numerical responses (red lines), the estimated periods $T_{is,num}$ are reported in Table 3. Actually, the vibration periods are smaller due the stiffer behaviour of HDRBs at small displacements. They can be estimated in the same way by considering the experimental responses. Results are reported in Table 3 at the column $T_{is,test}$. The global damping coefficient of the model is also reported in Table 3 (from which the constant c_0 have been evaluated considering and the dynamic stiffness of the system $k_0 + k_1$). Differently from the isolation period, it is not possible to evaluate the damping coefficient from experimental data, due to the non-zero displacement at the end of the free vibration motion. This is possible only if the motion oscillates around a zero position, thus if the loading phase is sufficiently fast, as shown in detail in the next section.

4.4. Simulation of test D3 with increased velocities

In order to show the influence of the lost displacement accumulated during the loading phase, Fig. 14 shows the response obtained by imposing a null lost displacement at the end of the loading phase (corresponding to the ideal case of a very fast loading phase). It is evident that the base isolated building oscillates around zero, thus both period and damping of the isolation system can be estimated in this case. In detail, the isolation period coincides with the time interval between the initial displacement and the successive positive peak, while for the damping the logarithmic decrement procedure can be used [25]. The best estimate is obtained by choosing the negative peaks giving a damping ratio of 0.15, very close to the model global damping reported in Table2.

To better understand the difference between the two responses of test D3 with real (Fig. 13) and ideal (Fig. 14) velocities, time histories of forces and energies involved during the oscillation are reported in Fig. 15, together with the force-displacements diagrams. For all the figures, the first column refers to the simulation of test D3, while the second one refers to the ideal fast case. It is evident that by increasing the velocity the force developed by the HDRBs and the related elastic energy are much higher, determining a different oscillation response. In terms of energy, as also shown in [26], the sum of the kinetic energy (green solid line) plus the total elastic energy (blue solid line) and the total dissipated energy (red solid line) provides the total input energy (black solid line). Moreover, the total dissipated energy is the sum of the contributions due to friction element as well as Maxwell and Kelvin models (red lines), while the total elastic energy is the sum of the contributions Maxwell and Kelvin models (blue lines). At the release instant, the input energy coincides with the elastic energy stored during the pushing phase by both the Maxwell and Kelvin models and, as expected, for the real velocity test the input energy is significantly lower and practically coincides with the Kelvin elastic energy (the Maxwell elastic energy is about zero). During the subsequent motion, the input energy remains constant while the kinetic, elastic and dissipated energies vary over time. It can be seen how the energy balance at the end of the motion is remarkably different between the two cases.

In order to further investigate this aspect, the numerical model has been used to simulate the test D3 with an increased velocity of the loading ramp. More in detail the loading ramp of test D3 has been imposed to the model with the actual velocity and with a velocity 10, 20, 40 and 100 times larger, as reported in Figs. 16a and 16b respectively.

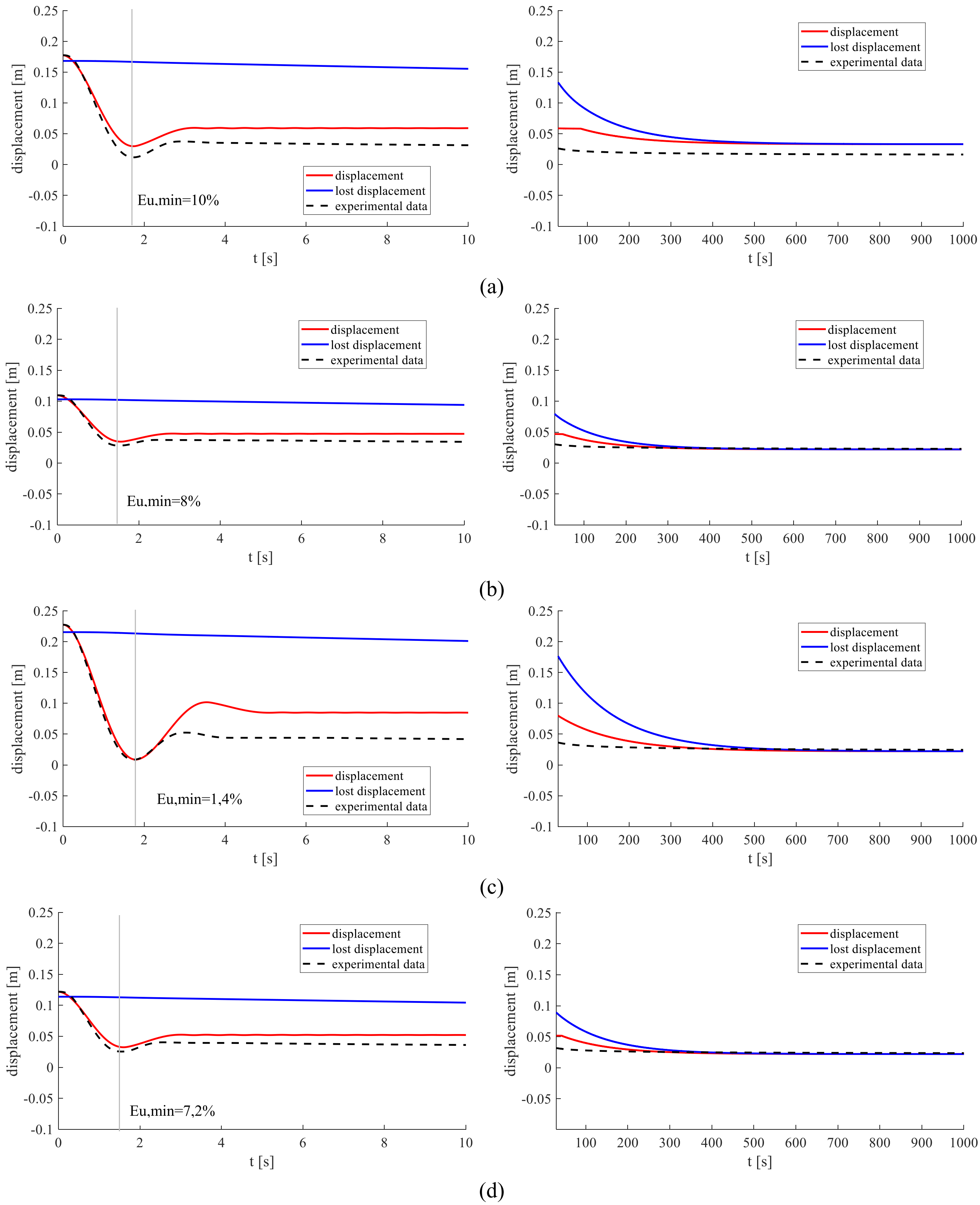

Fig. 12. Simulation of the response during the release phase of test D1(a), D2(b), D3(c) and D4(d).

Since the actual velocity is 0.175 m/s and correspond to a flow rate of 5 l/m, the increased velocity cases correspond to 1.75 m/s, 3.5 m/s, 7 m/s and 17.5 m/s and to flow rate of 50 l/min, 100 l/min, 200 l/min and 500 l/min respectively. It should be noted that all the considered velocities fall within the speed range between the OSR and HCC tests, both simulated through the proposed model for the isolators. It is confirmed that the initial lost displacement decreases as the velocity increases and that the system tends to oscillate around its initial position. It is evident that the latter case is very close to the ideal case, but a such a flow rate (500 l/m) can not be available outside a laboratory. More expensive systems compared to those used in the tests described in this article can reach flow rates of 50 or 100 l/min, and in rare cases, up

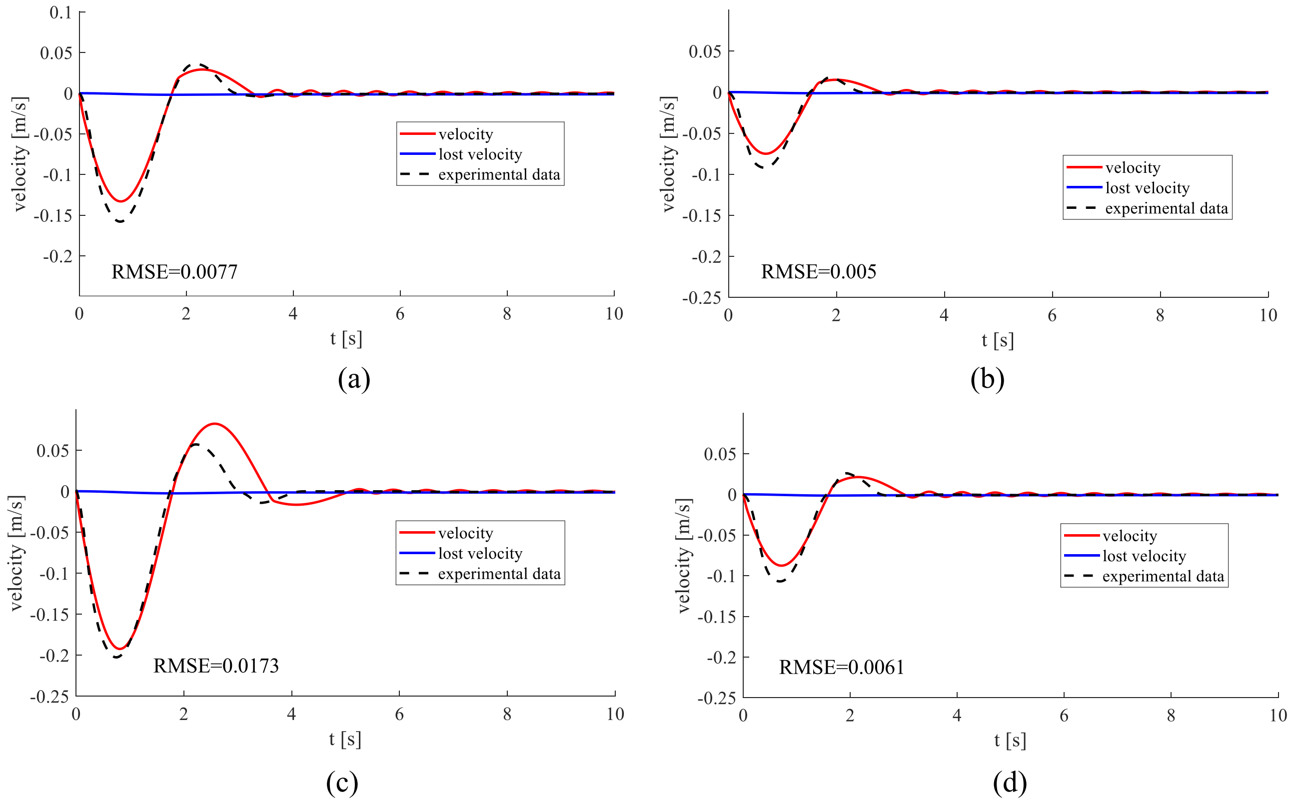

Fig. 13. Simulation of the response during the release phase of test D1 (a), D2 (b), D3 (c) and D4 (d).

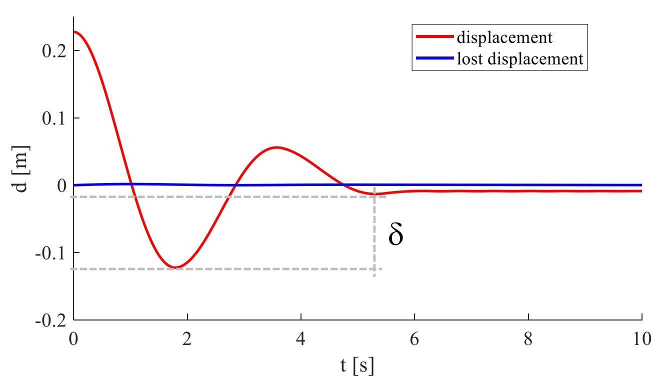

Fig. 14. Simulation of the response during the release phase of test D3 under the hypothesis of null lost displacement (ideal case) and evaluation of the response decrement δ.

to 200 l/min. Obviously, the obtained velocity values are related to the dimension of hydraulic jacks adopted, which in turn depend on the pushing forces and thus on the building dimensions. For smaller buildings with a fewer number of bearings and/or bearings with smaller dimensions, higher velocity values would be obtained for a given flow rate.

5. Conclusions

This article presented an overview of the experimental tests (quasi-static tests and push-and release tests) carried out on a strategic base-isolated building together with type tests carried out on a couple of HDRBs according to European standards on anti-seismic devices. Viscous effects have been highlighted and analysed in both the tests. Then, in order to interpretate the experimental tests a simple linear viscoelastic model has been proposed. First, a model simulating a single HDRB behaviour has been defined and its parameters computed based on type tests. The model has been then used to simulate in-situ tests considering the total numbers of elastomeric bearings and the friction contribution of the sliders. Based on the obtained results the following conclusion can be drown.

A very good agreement between experimental data and numerical simulation has been obtained, both for the short-term behaviour (free vibration) and long term behaviour (long term displacement), confirming the effectiveness of the simple proposed model as well as its calibration procedure based only on type tests (OSR and HCC tests) carried out on the bearings during the qualification process;

In detail, the model is able to compute the lost displacement accumulated during a slow loading ramp and causing the system to oscillate around a non-zero displacement decreasing over the time. The final residual displacement due to the friction force (once the long-term viscous effect fa vanished) can be also evaluated, demonstrating the small residual displacement of hybrid isolation systems based on HDRBs (after a sufficient period of time) if a low friction is guaranteed for the sliders.

Once the model parameters have been correctly computed form type test, the response to of the base-isolated building to any input can be simulated. As an example, in this paper faster loading ramps (usually not compatible with the capacity of hydraulic system for in-situ tests) have been applied, to show that the cumulated lost displacement decreases significantly leading to an higher elastic energy before the release and larger oscillations around the initial position of the structural systems. Both the isolation period and the damping coefficient of the isolation system can be estimated in this situation and compared with design values.

Since for a given flow rate, the resulting velocity depends on the area of the hydraulic jacks (i.e. the applied forces) for small buildings (thus small pushing forces), high loading velocities can be applied with conventional transportable hydraulic systems. Differently, for large buildings (like the CHIP building), the same velocities would require very

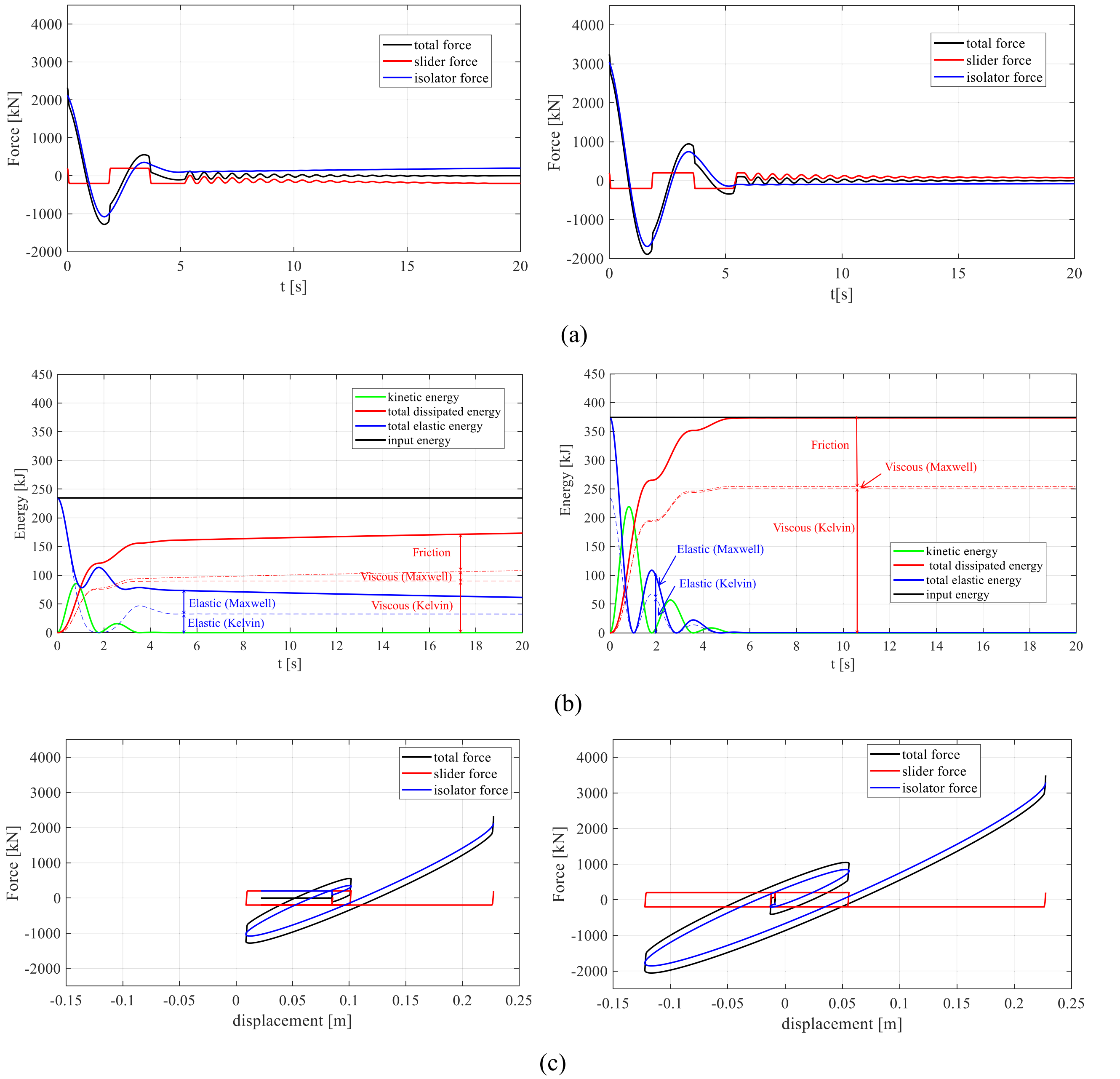

Fig. 15. Simulation of the response during the release phase of test D3 in left column and ideal case of test D3 in the right column, in terms of balance of forces (a), balance of energy (c) and force-displacement hysteresis loops (c).

large hydraulic capacities, thus expensive hydraulic systems. However, with the proposed model and the corresponding calibration procedure available, it is possible to use less expensive systems and interpret the results afterward, deriving the dynamic properties of the isolators under seismic conditions through the proposed simple model.

The response of the proposed model to seismic inputs coincides with the equivalent linear model suggested by seismic codes for this kind of isolation systems. However, it can also be used to simulate the response to slow actions, such as temperature variations.

CRediT authorship contribution statement

Andrea Dall'Asta: Writing – review & editing, Supervision, Methodology, Conceptualization. **Laura Ragni:** Writing – review & editing, Writing – original draft, Software, Methodology, Formal analysis, Data curation, Conceptualization. **Fabio Micozzi:** Writing – review & editing, Software, Methodology, Investigation, Formal analysis, Data curation, Conceptualization.

Acknowledgements

All persons who have made substantial contributions to the work reported in the manuscript (e.g., technical help, writing and editing assistance, general support), but who do not meet the criteria for authorship, are named in the Acknowledgements and have given us their written permission to be named. If we have not included an Acknowledgements, then that indicates that we have not received substantial contributions from non-authors.

Declaration of Competing Interest

The authors declare that they have no known competing financial

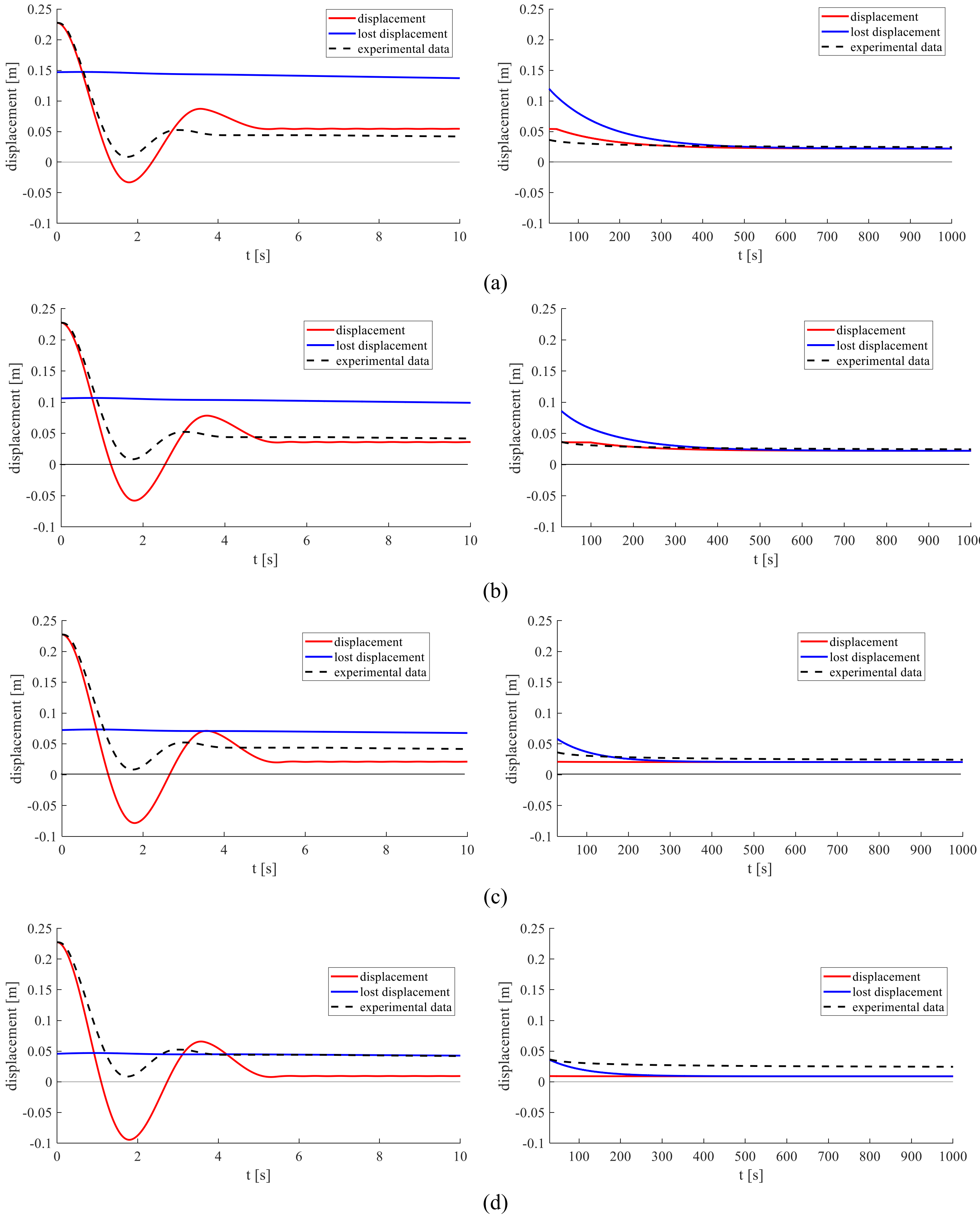

Fig. 16. Simulation of the response for different velocity of the loading phase: 10v (a), 20v (b), 40v (c) and 100v (d).

interests or personal relationships that could have appeared to influence the work reported in this paper.

Acknowledgements

The financial support for these tests provided by the Italian Department of Civil Protection is gratefully recognized. For the interpretation of tests, partial financial support was received by the Italian Department of Civil Protection, within the ReLUIS projects 2024–2026.

Data availability

Data will be made available on request.

References

[1] Dall'Asta A, Ragni L. Experimental tests and analytical model of high damping rubber dissipating devices. Eng Struct 2006;28(13):1874–84.
[2] Tubaldi E, Ragni L, Dall'Asta A, Ahmadi H, Muhr A. Stress softening behaviour of HDNR bearings: modelling and influence on the seismic response of isolated structures: stress softening behaviour of HDNR bearings. Earthq Eng Struct Dyn 2017.
[3] Grant DN, Fenves GL, Whittaker AS. Bidirectional modeling of high-damping rubber bearings. J Earthq Eng 2004;8(1):161–85.
[4] Osterlof R, Wentzel H, Kari L, Diercks N, Wollscheid D. Constitutive modeling of the amplitude and frequency dependency of filled elastomers utilizing a modified boundary surface model. Int J Solids Struct 2014;51:3431–8.
[5] De Domenico D, Losanno D, Vaiana N. Experimental tests and numerical modeling of full-scale unbonded fiber reinforced elastomeric isolators (UFREIs) under bidirectional excitation. Eng Struct 2023;274:115118.
[6] Giuliani GC. Structural design, analysis and full-scale tests of seismically isolated buildings. Eng Struct 1993;15(2):102–16.
[7] Bixio AR, Dolce M, Nigro D, Ponzo FC, Braga F, Nicoletti M. Repeatable dynamic release tests on a base-isolated building. J Earthq Eng 2001;5(3):369–93.
[8] Braga F, Laterza M. Field testing of low-rise base isolated building. Eng Struct 2004;26(11):1599–610.
[9] Athanasiou A, Oliveto G. Modelling Hybrid Base Isolation Systems for Free Vibration Simulations, 8th International Conference on Urban Earthquake Engineering (8CUEE) (March). Tokyo, Japan: Tokyo Institute of Technology; 2011. p. 7–8.
[10] Athanasiou A. Dynamic Identification of the Augusta Hybrid Base Isolated Building Using Data From Full Scale Push and Sudden Release Tests. Ph.D. Dissertation. Italy: University of Catania; 2015.
[11] Dall'Asta A, Leoni G, Micozzi F, Gioiella L, Ragni L. A resilience and robustness oriented design of base-isolated structures: The New Camerino University Research Center. Front Built Environ 2020;6(1):50.
[12] Dall'Asta A, Leoni G, Gioiella L, Micozzi F, Ragni L, Morici M, Scozzese F, Zona A. Push-and-release tests of a steel building with hybrid base isolation. Eng Struct 2022;72:114971.
[13] EN 15129:2009 Anti-seismic devices, European Committee for Standardization, Brussels, 2009.
[14] DM 17 gennaio 2018. NTC 2018: Norme Tecniche per le costruzioni (in Italian), 2018.
[15] Dall'Asta A, Ragni L. Dynamic systems with high damping rubber: nonlinear behaviour and linear approximation. Earthq Eng Struct Dyn 2008;37:1511–26.
[16] Zayas V., Mahin S. and Constantinou M.C. Seismic Isolation Standard For Continued Functionality. Technical Report: UCB/SEMM-2017/03.
[17] Payne AR. The dynamic properties of carbon black-loaded natural rubber vulcanizates. Part I. J Appl Polym Sci 1962;6:57–63. https://doi.org/10.1002/app.1962.070061906.
[18] Kingston JGR, Muhr AH. Effect of scragging on parameters in viscoplastic model for filled rubber. Plast, Rubber Compos 2011;40(4):161–8.
[19] Mullins L. Softening of rubber by deformation. Rubber Chem Technol 1969;42(1):339–62.
[20] Govindjee S, Simo J. Mullins effect and the strain amplitude dependence of the storage modulus. Int J Solids Struct 1992;29(14-15):1737–51.
[21] ASCE. 7-16 Minimum Design Loads and Associated Criteria for Buildings and Other Structures. Reston, VA: American Society of Civil Engineers; 2017.
[22] Dall'Asta A, Ragni L. Dynamic systems with high damping rubber: Nonlinear behaviour and linear approximation. Earthq Eng Struct Dyn 2008;37:1511–26.
[23] Kelly JM. Earthquake-Resistant Design With Rubber. 2nd edition. London: Springer; 1997.
[24] Leitman MJ, Fisher GMC. The Linear Theory of Viscoelasticity, Handbuch der Physik. Berlin-Heidelberg - New York: Springer; 1973. p. 1–123. VIa/3.
[25] A.K. Chopra, Dynamics of structures: theory and applications to earthquake engineering, Prentice Hall, 1995.
[26] Dall'Asta A, Ragni L. Nonlinear behaviour of dynamic systems with high damping rubber devices. Eng Struct 2008;30:3610–8.